https://doi.org/10.1016/j.ejphar.2015.12.011

Elsevier Editorial System(tm) for European Journal of Pharmacology

Manuscript Draft

Manuscript Number: EJP-42615R1

Title: Impairing effects of angiotensin-converting enzyme inhibitor Captopril on bone of normal mice

Article Type: Research Paper

Section/Category: Endocrine pharmacology

Keywords: Renin-angiotensin system; Angiotensin-converting enzyme inhibitor; Bone; Captopril; Bradykinin receptor; Angiotensin II

Corresponding Author: Dr. Yan Zhang, Ph.D

Corresponding Author's Institution: University of Shanghai for Science and Technology

First Author: Min Yang

Order of Authors: Min Yang; Chao Xia; Yan Song; Xi Zhao; Man-Sau Wong; Yan Zhang, Ph.D

Abstract: There are contradicting results about the effects of angiotensin-converting enzyme inhibitors (ACEIs) on bones. This study was aimed to investigate the effect of ACEI, Captopril, on bone metabolism and histology as well as the action of Captopril on skeletal renin-angiotensin system (RAS) and bradykinin receptor pathway in normal male mice. The urine, serum, tibias and femurs from normal control mice and Captopril-treated (10 mg/kg) mice were collected for biochemical, histological and molecular analyses after drug administration for eight weeks. The mice after the treatment with Captopril had a significant decrease of serum testosterone level. The histological measurements showed the loss of trabecular bone mass and trabecular bone number, and the breakage of trabecular bone network as well as the changes of chondrocyte zone at epiphyseal plate in Captopril-treated mice. The defect of Captopril on trabecular bone was reflected by the quantitative bio-parameters from micro-CT. The expression of renin receptor and bradykinin B2 receptor (B2R) was significantly up-regulated in tibia of mice upon to the Captopril treatment, which decreased the ratio of OPG/RANKL and the expression of osteoblastic factor RUNX2. Furthermore, Captopril treatment resulted in the increase of pAkt/Akt and pNFκB expression in tibia. The present study revealed the impairing effects of Captopril on bone via interfering with the circulating sex hormone level and B2R pathway, which suggests that the bone metabolism of patients need to be carefully monitored when being prescribed for ACEIs.

Impairing effects of angiotensin-converting enzyme inhibitor Captopril on bone of normal mice

Min Yang [a#], Chao Xia [a#], Yan Song [a], Xi Zhao [a], Man-Sau Wong [b], Yan Zhang [a,*]

[a] *School of Pharmacy, Nantong University, Nantong 226001, China.*

[b] *Department of Applied Biology and Chemical Technology, The Hong Kong Polytechnic University, Hung Hom, Kowloon, Hong Kong.*

# contributed equally to this work.

[*] Correspondence to Dr. Yan Zhang

Correspondence address: Qixiu Road 19, Nantong 226001, Jiangsu Province, China.

E-mail: riceandtiger@163.com

Tel: 86-0513-85051728

Fax: 86-0513-85051730

Abstract

There are contradicting results about the effects of angiotensin-converting enzyme inhibitors (ACEIs) on bones. This study was aimed to investigate the effect of ACEI, Captopril, on bone metabolism and histology as well as the action of Captopril on skeletal renin-angiotensin system (RAS) and bradykinin receptor pathway in normal male mice. The urine, serum, tibias and femurs from normal control mice and Captopril-treated (10 mg/kg) mice were collected for biochemical, histological and molecular analyses after drug administration for eight weeks. The mice after the treatment with Captopril had a significant decrease of serum testosterone level. The histological measurements showed the loss of trabecular bone mass and trabecular bone number, and the breakage of trabecular bone network as well as the changes of chondrocyte zone at epiphyseal plate in Captopril-treated mice. The defect of Captopril on trabecular bone was reflected by the quantitative bio-parameters from micro-CT. The expression of renin receptor and bradykinin B2 receptor (B2R) was significantly up-regulated in tibia of mice upon to the Captopril treatment, which decreased the ratio of OPG/RANKL and the expression of osteoblastic factor RUNX2. Furthermore, Captopril treatment resulted in the increase of pAkt/Akt and pNFκB expression in tibia. The present study revealed the impairing effects of Captopril on bone via interfering with the circulating sex hormone level and B2R pathway, which suggests that the bone metabolism of patients need to be carefully monitored when being prescribed for ACEIs.

Keywords: Renin-angiotensin system; Angiotensin-converting enzyme inhibitor; Bone; Captopril; Bradykinin receptor; Angiotensin II

1. Introduction

The renin-angiotensin system (RAS) plays a central role in the control of blood pressure and fluid balance within the body (Namazi et al., 2011). In addition to the systemic RAS, the emerging evidences revealed the expression and function of RAS in local tissue, namely tissue RAS, which is postulated to participate in various pathophysiologic processes (Inaba et al., 2011; Koïtka et al., 2010; Lau et al., 2004; Wong et al., 2010; Yung et al., 2011).

Recent in vivo studies showed the expression of RAS components in trabecular bone (Asaba et al., 2009; Izu et al., 2009; Zhang et al., 2014a; Zhang et al., 2014b), and in vitro study demonstrated the existence of angiotensin receptors in primary osteoblasts (Asaba et al., 2009), indicating the RAS components are expressed locally in bone microenvironment. The animal studies in our group demonstrated that the skeletal RAS was involved in osteoporosis induced by ageing (Gu et al., 2012a), and trabecular bone injuries of mice with either obstructive nephropathy (Gu et al., 2012b) or type 1 diabetes (Diao et al., 2014). Furthermore, the other studies identified the roles of local bone RAS in fracture healing (Garcia et al., 2010), the steroid-induced osteonecrosis (Zhang et al., 2014a), and the development of postmenopausal osteoporosis in ovariectomized animal models (Liu et al., 2011; Shimizu et al., 2008) as well as glucocorticoid-induced osteoporosis (Shuai et al., 2015). Therefore, the previous studies suggested that the local RAS exists in bone tissue and has a vital biological action on bone metabolism.

The main effector peptide angiotensin II (Ang II) in RAS is produced from Ang I

by the action of angiotensin-converting enzyme (ACE), a key molecule in RAS. ACE inhibitor (ACEI) could increase bone mineral density (BMD) and reduce fracture risk in patients (García-Testal et al., 2006; Lynn et al., 2006; Rejnmark et al., 2006). However, some clinical results showed that the application of ACEI did not have positive effects on bones (Stimpel et al., 1995), and even led to bone loss (Kwok et al., 2012; Masunari et al., 2008; Zhang et al., 2012b).

In animal studies, the ACEI treatment suppressed the estrogen deficiency-induced decrease in bone density (Shimizu et al., 2009), accelerated bone healing and remodeling (Garcia et al., 2010), and improved osteoporosis and hypertension (Asaba et al., 2009). While, our group recently elucidated that the treatment with ACEI, Captopril, significantly elevated the level of tartrate-resistant acid phosphatase in serum, and had a trend to decrease BMD and damage micro-architecture of trabecular bone in type 1 diabetic mice (Diao et al., 2014).

In view of the contradictory effects of ACEI on bone health, we are keen to know the effects of ACEI on bone tissue of normal mice at normotensive condition. This study was performed to investigate the effect of ACEI, Captopril, on bone mass, micro-architecture and histology, and the action of Captopril on skeletal RAS and bone metabolic regulators in normal male mice.

2. Materials and methods

2.1. Animal treatment

The 10-week-old male ICR mice (Slac Laboratory Animal, Shanghai, China) were randomly divided into normal control group (n = 7) and Captopril-treated group (10 mg/kg, i.g, n = 8). After the treatment for eight weeks, mean arterial blood pressure (MAP) was analysed by cannulation of the right carotid artery (Servomed, Hellige GmbH, Freiburg, Germany). The urine, serum, tibias and femurs were harvested for the biochemical, histological and molecular analyses. The protocol for animal study was reviewed and approved by the institution's Animal Ethics Committee at the Nantong University. Animals were maintained in accordance with the *Guide for the Care and Use of Laboratory Animals* (8^{th} edition, Institute of Laboratory Animal Resources on Life Sciences, National Research Council, National Academy of Sciences, Washington DC).

2.2. Serum and urine chemistries

The concentrations of calcium (Ca), phosphorus (P) and creatinine (Cr) in serum and urine were measured by standard colorimetric methods using a micro-plate reader (Bio-Tek, USA). The urinary level of Ca and P was corrected by the concentration of urine Cr. The serum levels of bone turnover markers, tartrate-resistant acid phosphatase 5b (TRAP), and procollagen type I N-terminal propeptide (PINP) were determined using sandwich ELISA kit purchased from Immunodiagnostic Systems

Ltd (Boldon, UK). The kit for serum testosterone was provided by ALPCO (USA).

2.3. Histological staining

The femurs were fixed in 4% formaldehyde/PBS (pH 7.2), decalcified in 0.5 M EDTA (pH 8.0), and embedded in paraffin by standard histological procedures. Serial sections of 3 μm were cut. Safranin O (Sigma-Aldrich) staining was performed, combining with fast green and counter stain by hematoxylin. Additionally, the Masson-Trichrome staining was also performed. Stained slides were visualized under microscope.

2.4. Tartrate-resistant acid phosphatase staining

Tartrate-resistant acid phosphatase (TRAP) staining was used for the identification of osteoclasts following the manufacturer's instructions (Sigma 387-A, St Louis, USA).

2.5. Micro-CT analysis

The femur without decalcification was fixed in a cylindrical plastic tube to prevent movement of the limb during measurement, and was scanned to obtain image. The distal femoral metaphysis was examined on 1.81 mm slab, corresponding to 173 slices, with a high-resolution micro viva-CT40 system (Scanco Medical, Bassersdorf, Switzerland). Trabecular bone was determined by a fixed threshold. The metaphyseal region of interest and trabecular compartments were isolated by hand-drawn contours based on 100 consecutive slices. The micro-architecture of trabecular bone was

assessed with direct three-dimensional (3D) methods by μCT Evaluation Program (Image Processing Language v. 5.0A, Scanco). The 3D parameters for morphology and structure of trabecular bone were obtained as the following: (1) bone volume over total volume (BV/TV); (2) connectivity density (Conn.D); (3) structure model index (SMI); (4) trabecular bone number (Tb.N); (5) trabecular bone thickness (Tb.Th); (6) trabecular bone separation (Tb.Sp); (7) the mean mineral density of total volume (BMD/TV); (8) bone surface over bone volume (BS/BV).

2.6. RT-PCR

The tibia RNA extraction was performed according to the TRIzol manufacturer's protocol (Invitrogen, Carlsbad, California, USA). The synthesis of complementary DNAs (cDNAs) was performed by reverse transcription reactions with 4 μg of total RNA using moloney murine leukemia virus reverse transcriptase (Invitrogen, Carlsbad, California, USA) with oligo $dT_{(15)}$ primers (Fermentas) as described by the manufacturer. The obtained cDNAs served as the template for the regular polymerase chain reaction using a DNA Engine (ABI). Glyceraldehyde-3-phosphate dehydrogenase (GAPDH) or β2-microglobulin (β2-M) as housekeeping gene was used to determine the relative expression of the target genes. The primer sequence used in this study was as previously described (Gu et al., 2012a).

2.7. Western blotting

The proteins from tibia were extracted in Laemmli buffer, followed by 5 min boiling

and centrifugation to obtain the protein lysis solution. After the determination on protein concentration by Bradford kits (Bio-Rad Laboratories, Hercules, CA, USA), 40 μg of protein were separated on 10% SDS-PAGE gel, transferred to nitrocellulose membranes (Bio-Rad Laboratories, Hercules, CA, USA). After blocking with 5% (w/v) nonfat dry milk in TBS and 0.1% (w/v) Tween 20 (TBST), the membranes were incubated with one of the following primary antibodies at dilutions ranging from 1:500 to 1:200 at 4℃ overnight: mouse anti-renin monoclonal antibody, goat anti-angiotensin II polyclonal antibody, goat anti-bradykinin B1R polyclonal antibody, goat anti-bradykinin B2R polyclonal antibody, goat anti-Akt1/2 polyclonal antibody, rabbit anti-pAkt1/2/3 polyclonal antibody, and rabbit anti-pNFκB polyclonal antibody. All the above primary antibodies were purchased from Santa Cruz Biotechnology (USA). After three washes with TBST, membranes were incubated with secondary immunoglobulins conjugated to IRDye 800CW Infrared Dye (LI-COR), including donkey anti-goat, anti-mouse and anti-rabbit IgG with the dilution of 1:15000. Blots were visualized by the Odyssey Infrared Imaging System (LI-COR Biotechnology, USA) and densitometrically assessed on target bands with Odyssey Application Software (version 3.0). The internal reference protein β-actin was used for correcting unequal loading using the mouse monoclonal anti-β-actin antibody (Sigma, USA).

2.8. Statistical analysis

The data in this study were reported as mean ± standard error of mean (S.E.M.). All statistical analyses were performed using PRISM version 4.0 (GraphPad). The

difference between groups was analyzed by Student's *t*-test. Difference with *P* value of less than 0.05 was considered statistically significant.

3. Results

3.1. Mean arterial blood pressure

The normal mice treated with the ACE inhibitor Captopril showed a significantly ($P < 0.05$) lower mean arterial pressure (64.6 ± 3.5 mmHg) when compared with non-treated controls (83.9 ± 3.8 mmHg).

3.2. Serum and urine biomarkers

The main minerals including calcium and phosphorous contained in bones were measured in serum and urine (Table 1). The mice treated with Captopril showed the decrease of serum calcium level ($P < 0.05$) and almost the two-fold increase of urinary calcium excretion ($P < 0.01$), while, the phosphorus levels in serum and urine were comparable between the normal control group and Captopril-treated group.

Table 1 Chemistries in serum and urine

	Serum Ca (mg/dl)	Serum P (mg/dl)	Urine Ca/Cr (mg/mg)	Urine P/Cr (mg/mg)
Control	10.39 ± 0.35	8.26 ± 0.19	0.121 ± 0.015	0.095 ± 0.023
Captopril	8.94 ± 0.27 [a]	8.08 ± 0.47	0.230 ± 0.014 [b]	0.102 ± 0.024

Values are expressed as means ± S.E.M., $n = 7$~8 in either group.

[a] $P < 0.05$ for the comparison with Control group

[b] $P < 0.01$ for the comparison with Control group

Ca, calcium; Cr, creatinine; P, phosphorus.

3.3. Bone turnover markers in serum

The treatment with Captopril decreased the serum level of testosterone ($P < 0.05$) as compared to that of control group (Table 2), but did not significantly changed the serum level of procollagen type I N-terminal propeptide (PINP), one of bone formation markers, or tartrate-resistant acid phosphatase (TRAP), one of bone resorption markers, even though there were a trend of decrease of both the two bone turnover markers in Captopril-treated group.

Table 2 Serum levels of sex hormone testosterone and bone turnover markers

	Testosterone (ng/ml)	TRAP (U/l)	PINP (ng/ml)
Control	15.7 ± 1.3	12.2 ± 0.9	154.9 ± 49.8
Captopril	11.2 ± 0.8 [a]	10.9 ± 0.6	116.0 ± 31.9

Values are expressed as means ± S.E.M., $n = 7$~8 in either group.

[a] $P < 0.05$ for the comparison with Control group

TRAP, tartrate-resistant acid phosphatase; PINP, procollagen type I N-terminal propeptide.

3.4. Histology of distal femoral end

Safranin O staining (Fig. 1A, B) and Masson-Trichrome staining (Fig. 1C-F) were conducted to observe the epiphyseal region of distal femoral end, including epiphyseal plate, upper epiphyseal cartilages and the secondary spongiosa zone. The loss of bone quantity and network connection of trabecular bone was observed at the secondary spongiosa zone of distal femurs of Captopril-treated mice (Fig. 1B, D) as

compared to normal control mice (Fig. 1A, C). Similarly, the thickness of the cartilages adjacent to the epiphyseal plate in treatment group was reduced (shown by purple arrow), suggesting the occurrence of delayed formation of new cartilages upper epiphyseal plate upon to Captopril treatment. The chondrocyte zone at growth plate of distal femoral end was magnified for observing the proliferation zone and hypertrophic zone shown by Masson-Trichrome staining (Fig. 1E, F). The morphology of the cells in proliferation zone was irregular and the thickness of the hypertrophic zone was reduced in the Captopril group (Fig. 1F) as compared to those of control group (Fig. 1E). Thus, both of the histological stainings revealed the remarkable bone abnormalities at the distal femoral end of mice administered with Captopril.

3.5. Tartrate-resistant acid phosphatase staining

In the normal control group, few osteoclasts could be identified in the trabecular bone area underneath growth plate of distal femoral end (Fig. 2, shown by blue arrow), whereas the distinct increase of osteoclasts number in this area was observed in Captopril-treated group.

3.6. Micro CT analysis

The profiles of 3D images (Fig. 3) clearly demonstrated the loss of trabecular bone mass and trabecular bone number as well as the breakage of cancellous bone at distal metaphysis of femur, and the 3D bone biological parameters (Table. 3) quantitatively

reflected these observed changes. The treatment with Captopril triggered the decrease of trabecular bone number (Tb.N) by 11.4%, connectivity density (Conn.D) by 23.5%, bone volume over total volume (BV/TV) by 17.0% and trabecular bone mineral density over total volume (BMD/TV) by 14.9%, and the increase of trabecular bone separation (Tb.Sp) by 25.2%, in distal femoral metaphysis as compared to those parameters of the control group. Notably, these changes of bone parameters on bone micro-architecture and bone mass were not statistically different between groups.

Table 3 Bone parameters of distal femoral end in normal control group and Captopril-treated group.

	Control	Captopril
BV/TV	0.358 ± 0.044	0.297 ± 0.023
Conn. D ($1/mm^3$)	818 ± 14	626 ± 72
SMI	1.68 ± 0.54	1.72 ± 0.07
Tb. N (1/mm)	7.0 ± 0.2	6.2 ± 0.3
Tb. Th (μm)	50.1 ± 5.1	46.9 ± 1.9
Tb. Sp (μm)	92.9 ± 10.2	116.3 ± 9.1
BMD/TV (mg HA/ccm)	255 ± 29	217 ± 16
BS/BV (1/mm)	40.3 ± 4.1	42.8 ± 1.7

Values are expressed as means ± S.E.M., n = 6~8. BV/TV: bone volume over total volume, Conn. D: connectivity density, SMI: structure model index, Tb.N: trabecular bone number, Tb.Th: trabecular bone thickness, Tb.Sp: trabecular bone separation, BMD/TV: bone mineral density over total volume, BS/BV: bone surface over bone volume.

3.7. mRNA expression of skeletal RAS components

The mRNA expression of RAS components, including angiotensin-converting enzyme (ACE), angiotensin type 1 receptor and renin receptor (Renin-R), was measured in tibia (Fig. 4). The treatment of Captopril significantly up-regulated the mRNA expression of renin receptor ($P < 0.01$), but did not alter the mRNA expression of ACE and angiotensin type 1 receptor.

3.8. Protein expression of skeletal RAS components

The protein expression of renin, angiotensin II (Ang II), bradykinin B1 receptor (B1R) and B2 receptor (B2R) was determined in tibia (Fig. 5). The mice after treatment with Captopril showed lower expression of renin (Fig. 5B, $P < 0.01$) and higher expression of B2R ($P < 0.05$) than those of mice without drug treatment. In addition, the Captopril treatment did not alter the protein expression of Ang II and B1R.

3.9. mRNA expression of key regulators for bone metabolism

The maturation and formation of osteoclasts are mainly regulated by the balance of extracellular levels of OPG and RANKL secreted by osteoblasts, and runt-related transcription factor 2 (RUNX2) is a major regulator for osteoblastic function, thus, the ratio of OPG/RANKL and the mRNA expression of RUNX 2 in tibia were determined in this study (Fig. 6). The ratio of OPG/RANKL mRNA expression ($P < 0.05$) and the mRNA expression of RUNX2 ($P < 0.01$) were significantly decreased in

Captopril group.

3.10 Protein expression of pAkt and pNFκB

The expression of downstream proteins (pAkt and pNFκB) associated with B2R activation was determined (Fig. 7). Captopril treatment caused 95% of increase in the expression of pAkt/Akt ($P < 0.01$) in tibia. When checked for the phosphorylation of NFκB, we found that the Captopril-treated mice showed significant upregulation of pNFκB as compared to that of vehicle-treated mice ($P < 0.05$).

4. Discussion

Since high blood pressure is associated with the risk of bone loss (Cappuccio et al., 1999), the attention should be highly paid to the effects of agents used in the treatment for cardiac-vascular diseases on bone health and possible intervention approaches. Additionally, angiotensin-converting enzyme inhibitors (ACEIs) are currently in wide use for the treatment of diabetes complications, like diabetes-induced heart diseases (Cheng et al., 2014) and diabetes nephropathy (Impellizzeri et al., 2014), moreover, osteoporosis is often associated with diabetes (Hofbauer et al., 2007). Therefore, it is important to clarify the impacts of ACEIs on bone metabolism. In this study, we investigated the effects of one classical ACEI, Captopril, on bone metabolism, the local renin-angiotensin system (RAS) and bradykinin receptor pathway in bone tissue of normal mice with normotension.

Based on the study where reported that the OVX rats were administered with Captopril at dosage of 1 or 5 mg/kg (Liu et al., 2011), the dosage for mouse could be calculated as 1-5 mg/kg × 2 (conversion factor from rat to mouse) = 2-10 mg/kg. Thus, the current dosage for mice (10 mg/kg) used in this study is comparable and acceptable for pharmacological study.

Previously, most of clinical studies demonstrated that ACEI could increase bone mineral density (BMD) and reduce fracture risk (García-Testal et al., 2006; Ghosh and Majumdar, 2014; Lynn et al., 2006; Rejnmark et al., 2006). The treatment with Enalapril improved osteoporosis of Tsukuba hypertensive mouse (Asaba et al., 2009), and the treatment with Captopril (1 or 5 mg/kg) increased the trabecular bone area of

lumbar vertebrae (L4) and improved the bone mechanical properties by increasing break stress and elastic modulus of L5 in ovariectomized rats (Liu et al., 2011). Similarly, Perindopril partially reversed the glucocorticoid-induced osteoporosis in rabbits (Zhang et al., 2014a). While, this study showed that Captopril, which inhibits the conversion of angiotensin I (Ang I) to the active hormone Ang II, had the potential effects on damaging the micro-architecture of trabecular bone and enhancing the number of matured osteoclasts in distal metaphysis of femur in normal male mice, which was also found in type 1 diabetic mice after treatment with Captopril (Diao et al., 2014), moreover, Captopril destroyed the chondrocyte zone of epiphyseal plate in femur, in concert with the in vivo study which revealed that the inhibition of RAS attenuated Ang II-induced hypertrophic differentiation of chondrocytes in growth plate of mouse tibia (Kawahata et al., 2015). These effects were also in agreement with what have been recently reported in clinical studies utilizing ACEIs (Kwok et al., 2012; Masunari et al., 2008; Stimpel et al., 1995; Zhang et al., 2012b), indicating a potential adverse effect of Captopril, even all ACEIs, on bone metabolism.

The impairments of Captopril on skeleton are surprising, since ACE is the key enzyme producing Ang II. A possible reason may be attributed to the decrease of blood pressure of normal mice in response to Captopril. The mean arterial blood pressure (MAP) determines intramedullar pressure that is a driving force for transcortical interstitial fluid (ISF) flow (Garcia et al., 2010), and an increased intramedullar pressure has been shown to improve bone quality due to an increased ISF flow (Hillsley and Frangos, 1994). While, whether there are direct

pharmacological actions of Captopril contributing to its detrimental effects on bone of normal mice, besides the Captopril-associated reduction of MAP, was specially investigated in this study.

The regulation of ACE inhibitors on sex hormones may another cause to explain its potential deterioration on bone tissue. This study found that Captopril decreased the circulating level of testosterone in male mice, in accordance with previous report that Lisinopril significantly decreased free testosterone in men and increased sex hormone-binding globulin in women over a 6-month period of treatment (Koshida et al., 1998). In addition, a cross-sectional study performed on older Chinese men found that the use of ACEI was associated with the lower level of serum dehydroepiandrosterone (Kwok et al., 2010). The mechanisms have not yet been fully revealed and more studies need to be carried out to clarify the relationship between the RAS and sex hormones level.

It is well known that the high activity of skeletal RAS, especially the increased production of Ang II, the bioactive peptide within RAS, would lead to bone injuries. This study showed that the use of Captopril did not change the expression of ACE, Ang II, and angiotensin type 1 receptor in bone tissue, suggesting the RAS classical pathway, so-called ACE/Ang II/ angiotensin type 1 receptor, was maintained at the normal level. Although the short-term therapy by ACEI was associated with the decreased level of Ang II, there were some evidences showing that the long-term inhibition by ACEI resulted in a return of Ang II to the baseline level, namely 'ACE escape' (Zhang et al., 2012b). This study demonstrated that the long-term application

of Captopril in normal mice resulted in the down-regulation of renin and the up-regulation of renin receptor. How the alteration of renin/renin receptor pathway to affect bone metabolism still needs to be further studied as this pathway was involved in kinds of local tissue diseases (Zhang et al., 2012a).

ACE inhibitors act not only on the RAS, but also on the kinin-kallikrein system (KKS) by suppressing degradation of bradykinin (Zhang et al., 2012b), which is the major effector peptide in KKS and is one of substrates by ACE. Bradykinin normally displays its effects by activating two seven transmembrane G protein-coupled receptors, named B1 (B1R) and B2 (B2R). It was reported that bradykinin is capable of decreasing the differentiation of osteoblasts with concomitant increasing the maturation of osteoclasts, consequently stimulating bone resorption and reducing BMD (Gonçalves-Zillo et al., 2013; Souza et al., 2013; Srivastava et al., 2014). The present study showed that Captopril induced the up-regulation of B2R protein expression, which may contribute to the impairing effects of Captopril on bone. Additionally, it was elucidated that angiotensin type 1 receptor and B2R communicate directly with each other by forming stable heterodimers, thereby causing increased activation of G alpha(q) and G alpha(i) proteins, the two major signaling proteins triggered by angiotensin type 1 receptor (AbdAlla et al., 2000), thus, whether the Captopril-induced increase in B2R expression activates the downstream pathway of angiotensin type 1 receptor is worth being investigated by further in depth studies.

In the next analysis for confirming the involvement of B2R signaling pathway in the process of Captopril-induced bone impairment, the protein expression of pAkt and

pNFκB was measured in bone tissue. Mounting evidences have shown that bradykinin activates its downstream proteins, including the phosphorylation of Akt and then NFκB, to influence the osteoblasts differentiation, stimulate osteoclasts formation and regulate the expression of a wide array of inducible genes, which finally produce negative effects on bone metabolism (Srivastava et al., 2014; Uchida et al., 2012). This study reported that the treatment with Captopril dramatically up-regulated the protein expression of pAkt and pNFκB, suggesting the crucial role of B2R/Akt/NFκB cascade in Captopril-induced bone deteriorations. Thus, the regulation of Captopril on B2R signaling pathway might well explain the observed increase of TRAP-positive osteoclast amount, the decrease of ratio of OPG/RANKL and the down-regulation of RUNX2 in bone tissue.

5. Conclusions

The present study demonstrated that the treatment with ACEI Captopril had potentially detrimental effects on trabecular bone of normal mice. The possible underlying mechanism for the damages of Captopril on bone may be attributed to the decreased level of serum testosterone and the activation of B2R/Akt/NFκB cascade in local bone tissue. The research studies need to be further performed to clarify the influences of ACEIs on bone health as this might be of closely clinical relevance when initiating antihypertensive therapy, particularly in hypertensive women who typically have a concomitant rapid onset of bone loss after menopause, and it is also an important consideration when prescribing ACEIs for those who suffering from

diabetes complications.

Acknowledgements

This work was sponsored by National Natural Science Foundation of China (No. 81202894).

Conflict of interest

The authors declare that there are no conflicts of interest.

References

AbdAlla, S., Lother, H., Quitterer, U., 2000. AT1-receptor heterodimers show enhanced G-protein activation and altered receptor sequestration. Nature. 2000, 407, 94-98.

Asaba, Y., Ito, M., Fumoto, T., Watanabe, K., Fukuhara, R., Takeshita, S., Nimura, Y., Ishida, J., Fukamizu, A., Ikeda, K., 2009. Activation of renin-angiotensin system induces osteoporosis independently of hypertension. J. Bone. Miner. Res. 24, 241-250.

Cappuccio, F.P., Meilahn, E., Zmuda, J.M., Cauley, J.A., 1999. High blood pressure and bone-mineral loss in elderly white women: a prospective study. Study of Osteoporotic Fractures Research Group. Lancet. 354, 971-975.

Cheng, J., Zhang, W., Zhang, X., Han, F., Li, X., He, X., Li, Q., Chen, J., 2014. Effect of angiotensin-converting enzyme inhibitors and angiotensin II receptor blockers on all-cause mortality, cardiovascular deaths, and cardiovascular events in patients with diabetes mellitus: a meta-analysis. JAMA. Intern. Med. 174, 773-785.

Diao, T.Y., Pan, H., Gu, S.S., Chen, X., Zhang, F.Y., Wong, M.S., Zhang, Y., 2014. Effects of angiotensin-converting enzyme inhibitor, captopril, on bone of mice with streptozotocin-induced type 1 diabetes. J. Bone. Miner. Metab. 32, 261-270.

Garcia, P., Schwenzer, S., Slotta, J.E., Scheuer, C., Tami, A.E., Holstein, J.H., Histing, T., Burkhardt, M., Pohlemann, T., Menger, M.D., 2010. Inhibition of angiotensin-converting enzyme stimulates fracture healing and periosteal callus formation - role of a local renin-angiotensin system. Br. J. Pharmacol. 159,

1672-1680.

García-Testal, A., Monzó, A., Rabanaque, G., González, A., Romeu, A., 2006. Evolution of the bone mass of hypertense menopausal women in treatment with fosinopril. Med. Clin. (Barc). 127, 692-694.

Ghosh, M., Majumdar, S.R., 2014. Antihypertensive medications, bone mineral density, and fractures: a review of old cardiac drugs that provides new insights into osteoporosis. Endocrine. 46, 397-405.

Gonçalves-Zillo, T.O., Pugliese, L.S., Sales, V.M., Mori, M.A., Squaiella-Baptistão, C.C., Longo-Maugéri, I.M., Lopes, J.D., de Oliveira, S.M., Monteiro, A.C., Pesquero, J.B., 2013. Increased bone loss and amount of osteoclasts in kinin B1 receptor knockout mice. J. Clin. Periodontol. 40, 653-660.

Gu, S.S., Zhang, Y., Li, X.L., Wu, S.Y., Diao, T.Y., Hai, R., Deng, H., 2012a. Involvement of the skeletal renin-angiotensin system in age-related osteoporosis of ageing mice. Biosci. Biotechnol. Biochem. 76, 1367-1371.

Gu, S.S., Zhang, Y., Wu, S.Y., Diao, T.Y., Gebru, Y.A., Deng, H., 2012b. Early molecular responses of bone to obstructive nephropathy induced by unilateral ureteral obstruction in mice. Nephrology, 17, 767-773.

Hillsley, M.V., Frangos, J.A., 1994. Bone tissue engineering: the role of interstitial fluid flow. Biotechnol. Bioeng. 43, 573–581.

Hofbauer, L.C., Brueck, C.C., Singh, S.K., Dobnig, H., 2007. Osteoporosis in patients with diabetes mellitus. J. Bone. Miner. Res. 22, 1317-1328.

Impellizzeri, D., Esposito, E., Attley, J., Cuzzocrea, S., 2014. Targeting inflammation:

new therapeutic approaches in chronic kidney disease (CKD). Pharmacol. Res. 81, 91-102.

Inaba, S., Iwai, M., Furuno, M., Kanno, H., Senba, I., Okayama, H., Mogi, M., Higaki, J., Horiuchi, M., 2011. Role of angiotensin-converting enzyme 2 in cardiac hypertrophy induced by nitric oxide synthase inhibition. J. Hypertens. 29, 2236-2245.

Izu, Y., Mizoguchi, F., Kawamata, A., Hayata, T., Nakamoto, T., Nakashima, K., Inagami, T., Ezura, Y., Noda, M., 2009. Angiotensin II type 2 receptor blockade increases bone mass. J. Biol. Chem. 284, 4857-4864.

Kawahata, H., Sotobayashi, D., Aoki, M., Shimizu, H., Nakagami, H., Ogihara, T., Morishita, R., 2015. Continuous infusion of angiotensin II modulates hypertrophic differentiation and apoptosis of chondrocytes in cartilage formation in a fracture model mouse. Hypertens. Res. 38, 382-393.

Koïtka, A., Cao, Z., Koh, P., Watson, A.M.D., Sourris, K.C., Loufrani, L., Soro-Paavonen, A., Walther, T., Woollard, K.J., Jandeleit-Dahm, K.A., Cooper, M.E., Allen, T.J., 2010. Angiotensin II subtype 2 receptor blockade and deficiency attenuate the development of atherosclerosis in an apolipoprotein E-deficient mouse model of diabetes. Diabetologia. 53, 584-592.

Koshida, H., Takeda, R., Miyamori, I., 1998. Lisinopril decreases plasma free testosterone in male hypertensive patients and increases sex hormone binding globulin in female hypertensive patients. Hypertens. Res. 21, 279-282.

Kwok, T., Leung, J., Zhang, Y.F., Bauer, D., Ensrud, K.E., Barrett-Connor, E., Leung, P.C.; Osteoporotic Fractures in Men (MrOS) Research Group., 2012. Does the use of

ACE inhibitors or angiotensin receptor blockers affect bone loss in older men? Osteoporos. Int. 23, 2159-2167.

Kwok, T., Ohlsson, C., Vandenput, L., Tang, N., Zhang, Y.F., Tomlinson, B., Leung, P.C., 2010. ACE inhibitor use was associated with lower serum dehydroepiandrosterone concentrations in older men. Clin. Chim. Acta. 411, 1122-1125.

Lau, T., Carlsson, P.O., Leung, P.S., 2004. Evidence for a local angiotensin-generating system and dose-dependent inhibition of glucose-stimulated insulin release by angiotensin II in isolated pancreatic islets. Diabetologia. 47, 240-248.

Liu, Y.Y., Yao, W.M., Wu, T., Xu, B.L., Chen, F., Cui, L., 2011. Captopril improves osteopenia in ovariectomized rats and promotes bone formation in osteoblasts. J. Bone. Miner. Metab. 29, 149-158.

Lynn, H., Kwok, T., Wong, S.Y., Woo, J., Leung, P.C., 2006. Angiotensin converting enzyme inhibitor use is associated with higher bone mineral density in elderly Chinese. Bone. 38, 584-588.

Masunari, N., Fujiwara, S., Nakata, Y., Furukawa, K., Kasagi, F., 2008. Effect of angiotensin converting enzyme inhibitor and benzodiazepine intake on bone loss in older Japanese. Hiroshima. J. Med. Sci. 57, 17-25.

Namazi, S., Ardeshir-Rouhani-Fard, S., Abedtash, H., 2011. The effect of renin angiotensin system on tamoxifen resistance. Med. Hypotheses. 77, 152-155.

Rejnmark, L., Vestergaard, P., Mosekilde, L., 2006. Treatment with beta-blockers, ACE inhibitors, and calcium-channel blockers is associated with a reduced fracture

risk: a nationwide case-control study. J. Hypertens. 24, 581-589.

Shimizu, H., Nakagami, H., Osako, M.K., Hanayama, R., Kunugiza, Y., Kizawa, T., Tomita, T., Yoshikawa, H., Ogihara, T., Morishita, R., 2008. Angiotensin II accelerates osteoporosis by activating osteoclasts. FASEB. J. 22, 2465-2475.

Shimizu, H., Nakagami, H., Osako, M.K., Nakagami, F., Kunugiza, Y., Tomita, T., Yoshikawa, H., Rakugi, H., Ogihara, T., Morishita, R., 2009. Prevention of osteoporosis by angiotensin-converting enzyme inhibitor in spontaneous hypertensive rats. Hypertens. Res. 32, 786-790.

Shuai, B., Yang, Y.P., Shen, L., Zhu, R., Xu, X.J., Ma, C., Lv, L., Zhao, J., Rong, J.H., 2015. Local renin-angiotensin system is associated with bone mineral density of glucocorticoid-induced osteoporosis patients. Osteoporos. Int. 26, 1063-1071.

Souza, P.P., Brechter, A.B., Reis, R.I., Costa, C.A., Lundberg, P., Lerner, U.H., 2013. IL-4 and IL-13 inhibit IL-1β and TNF-α induced kinin B1 and B2 receptors through a STAT6-dependent mechanism. Br. J. Pharmacol. 169, 400-412.

Srivastava, S., Sharma, K., Kumar, N., Roy, P., 2014. Bradykinin regulates osteoblast differentiation by Akt/ERK/NFκB signaling axis. J. Cell. Physiol. 229, 2088-2105.

Stimpel, M., Jee, W.S., Ma, Y., Yamamoto, N., Chen, Y., 1995. Impact of antihypertensive therapy on postmenopausal osteoporosis: effects of the angiotensin converting enzyme inhibitor moexipril, 17beta-estradiol and their combination on the ovariectomy-induced cancellous bone loss in young rats. J. Hypertens. 13, 1852-1856.

Uchida, Y., Endoh, T., Tazaki, M., Sueishi, K., 2012. Chronic bradykinin treatment alters 1α,25-dihydroxyvitamin D3-induced calcium current modulation in

pre-osteoblasts. Cell. Calcium. 51, 383-392.

Wong, W.T., Tian, X.Y., Xu, A., Ng, C.F., Lee, H.K., Chen, Z.Y., Au, C.L., Yao, X., Huang, Y., 2010. Angiotensin II type 1 receptor-dependent oxidative stress mediates endothelial dysfunction in type 2 diabetic mice. Antioxid. Redox. Signal. 13, 757-768.

Yung, L.M., Wong, W.T., Tian, X.Y., Leung, F.P., Yung, L.H., Chen, Z.Y., Yao, X., Lau, C.W., Huang, Y., 2011. Inhibition of renin-angiotensin system reverses endothelial dysfunction and oxidative stress in estrogen deficient rats. PLoS. One. 6, e17437.

Zhang, Y., Wang, K., Song, Q., Liu, R., Ji, W., Ji, L., Wang, C., 2014a. Role of the local bone renin-angiotensin system in steroid-induced osteonecrosis in rabbits. Mol. Med. Rep. 9, 1128-1134.

Zhang, Y., Wang, Y., Chen, Y., Deb, D.K., Sun, T., Zhao, Q., Li, Y.C., 2012a. Inhibition of renin activity by aliskiren ameliorates diabetic nephropathy in type 1 diabetes mouse model. J. Diabetes. Mellitus. 2, 353-360.

Zhang, Y.F., Qin, L., Leung, P.C., Kwok, T.C., 2012b. The effect of angiotensin-converting enzyme inhibitor use on bone loss in elderly Chinese. J. Bone. Miner. Metab. 30, 666-673.

Zhang, Y.T., Wang, K.Z., Zheng, J.J., Shan, H., Kou, J.Q., Liu, R.Y., Wang, C.S., 2014b. Glucocorticoids activate the local renin-angiotensin system in bone: possible mechanism for glucocorticoid-induced osteoporosis. Endocrine. 47, 598-608.

Figure legends

Fig. 1. Histological images of distal femoral end. A-B, Safranin O staining (Magnification, ×50), C-D, Masson-Trichrome staining (Magnification, ×100). The chondrocyte zone within the red elliptical line at growth plate (C, D) was magnified to be shown as E and F, respectively (Magnification, ×200). The cartilages adjacent to the epiphyseal plate were shown by the arrows with solid line (A, B).

Fig. 2. Tartrate-resistant acid phosphatase staining (Magnification, ×200) for osteoclasts (arrows in blue) in distal metaphysis of femur.

Fig. 3. Three-dimensional images reconstructed from Micro-CT analysis on the trabecular bone microarchitecture of distal femoral metaphysis.

Fig. 4. mRNA expression of RAS components in tibia (A), and the densitometric quantification for RT-PCR (B). ACE, angiotensin-converting enzyme; AT1R, angiotensin type 1 receptor; Renin-R, renin receptor. Values are expressed as means ± S.E.M., n = 7~8. ** $P < 0.01$, versus Control group.

Fig. 5. Protein expression of renin, angiotensin II (Ang II) and bradykinin receptors in tibia (A) and the densitometric quantification for Western blotting (B). Values are expressed as means ± S.E.M., n = 7~8. * $P < 0.05$, ** $P < 0.01$, versus Control group.

Fig. 6. mRNA expression of OPG, RANKL and RUNX2 in tibia (A), and the quantitative ratio of OPG/RANKL and the densitometric quantification for RUNX2 (B). OPG, osteoprotegerin; RANKL, receptor activator of nuclear factor-κB ligand; RUNX2, runt-related transcription factor 2. Values are expressed as means ± S.E.M., n = 7~8. * $P < 0.05$, ** $P < 0.01$, versus Control group.

Fig. 7. Protein expression of pAkt, Akt and pNFκB in tibia (A) and the densitometric quantification for Western blotting (B). Values are expressed as means ± S.E.M., n = 7~8. * $P < 0.05$, ** $P < 0.01$, versus Control group.

Figure 1

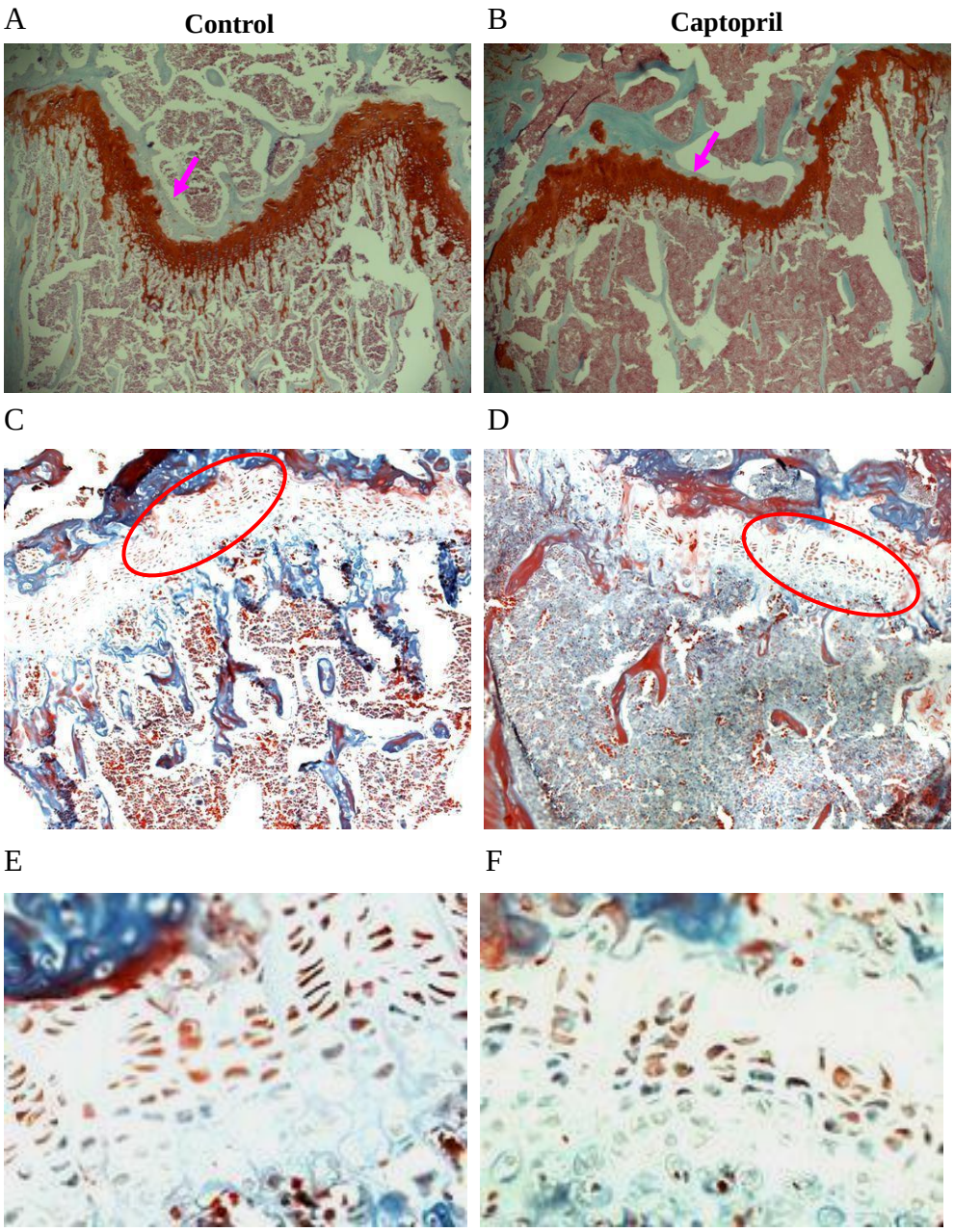

Figure 2

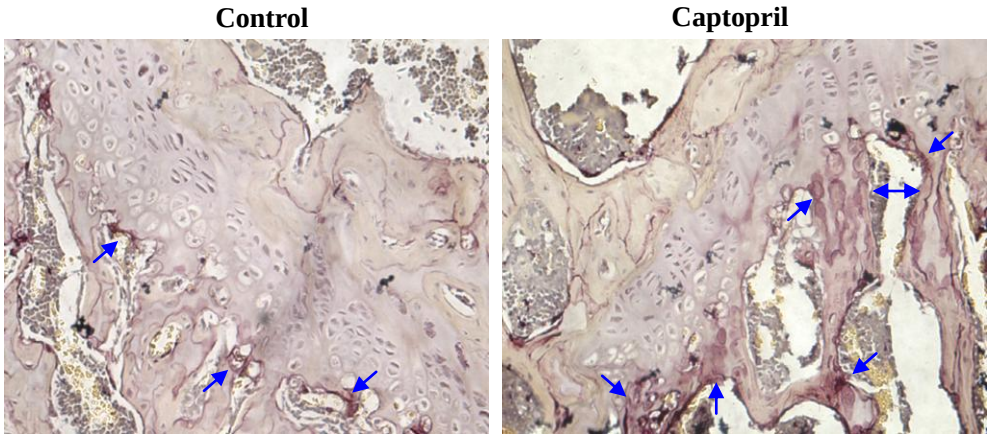

Figure 3

Control **Captopril**

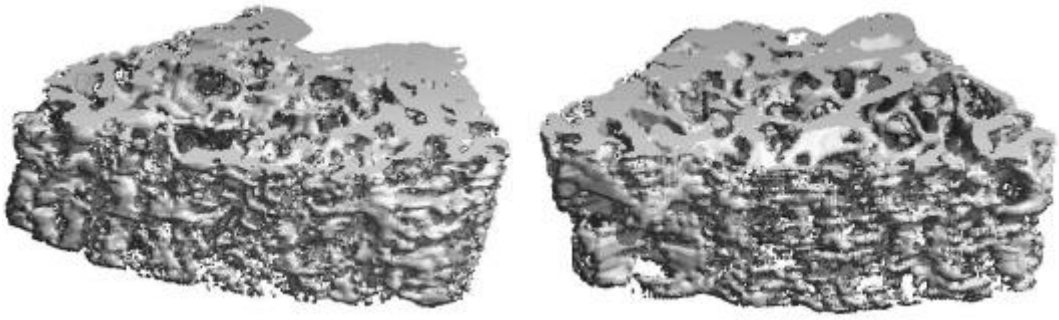

Figure 4

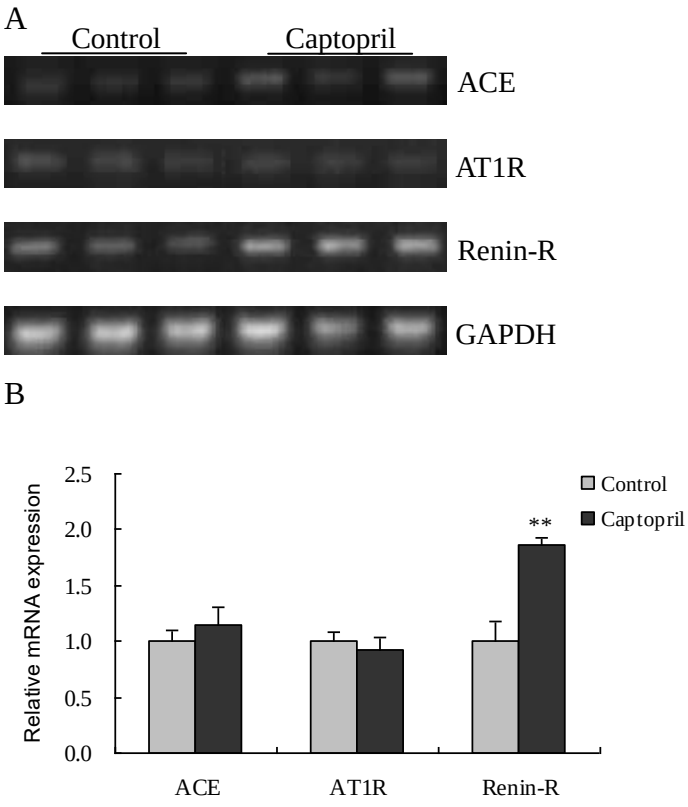
A
Control
Captopril
ACE
AT1R
Renin-R
GAPDH
B
Relative mRNA expression
2.5
2.0
1.5
1.0
0.5
0.0
Control
Captopril
**
ACE
AT1R
Renin-R

Figure 5

A

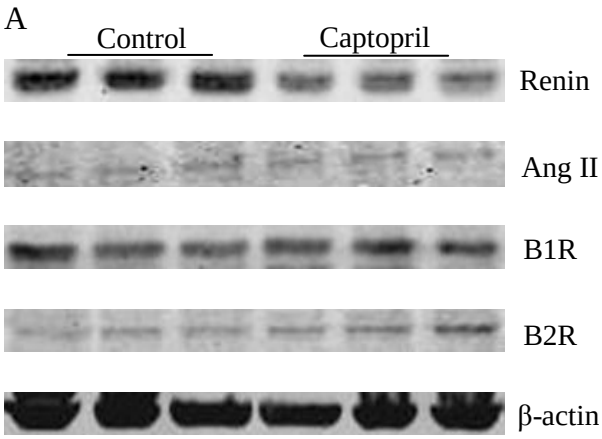
Control
Captopril
Renin
Ang II
B1R
B2R
β-actin

B

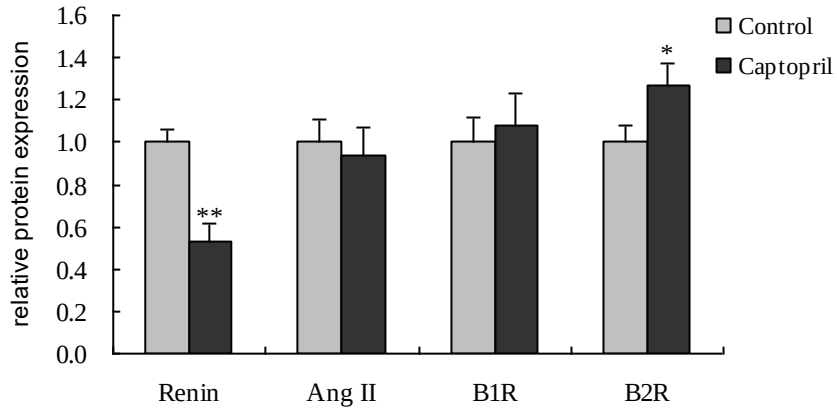
relative protein expression
1.6
1.4
1.2
1.0
0.8
0.6
0.4
0.2
0.0
**
*
Control
Captopril
Renin
Ang II
B1R
B2R

Figure 6

A

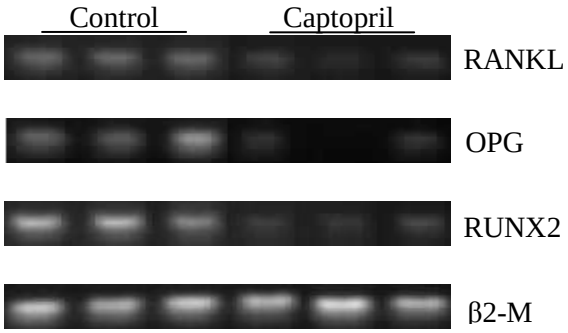
Control
Captopril
RANKL
OPG
RUNX2
β2-M

B

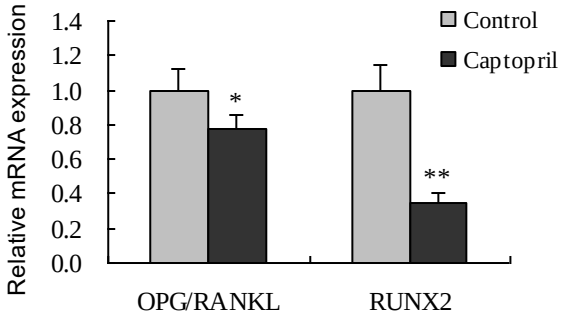
Relative mRNA expression
1.4
1.2
1.0
0.8
0.6
0.4
0.2
0.0
Control
Captopril
*
**
OPG/RANKL
RUNX2

Figure 7

A

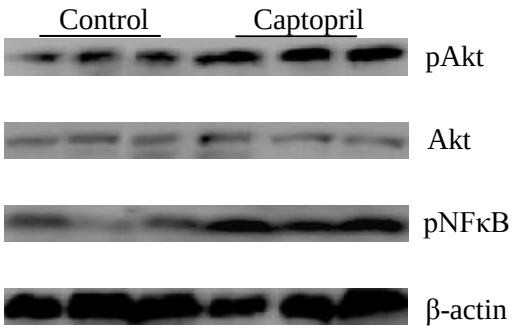
Control
Captopril
pAkt
Akt
pNFκB
β-actin

B

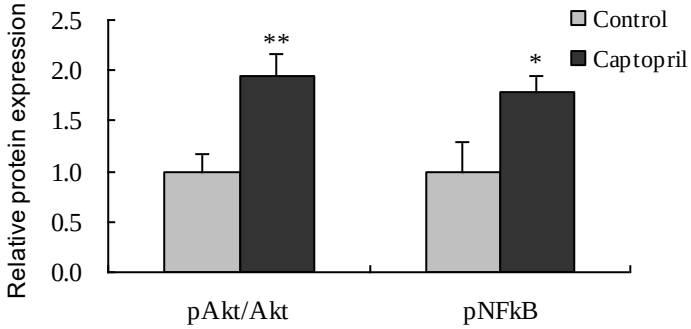
Relative protein expression
2.5
2.0
1.5
1.0
0.5
0.0
**
*
Control
Captopril
pAkt/Akt
pNFkB